Version of Record: https://www.sciencedirect.com/science/article/pii/S2214714422006122
Manuscript_07a547c5b43eab2798ba32d918fd59c4

Revealing the role of supernatant and granular sludge fractions on granular anaerobic membrane bioreactor fouling

Lucie Sanchez[a,b], Geoffroy Lesage[a*], Yasar Onur Demiral[b,c], Ignasi Rodriguez-Roda[b], Marc Heran[a], Gaetan Blandin[b]

[a] Institut Européen des Membranes (IEM), Université de Montpellier, CNRS, ENSCM, Montpellier, France

[b] LEQUIA, Institute of the Environment, University of Girona, Spain

[c] Dokuz Eylül University, The Graduate School of Natural and Applied Sciences, Tinaztepe Campus, Izmir, Turkey

*Corresponding author (e-mail: geoffroy.lesage@umontpellier.fr)

ABSTRACT

In order to design efficient fouling mitigation strategies in granular anaerobic membrane bioreactors (G-AnMBR), foulant characteristics and their role have to be thoroughly investigated. Raw mixed liquor of G-AnMBR was split by sieving into granules and supernatant fractions at 0.125 mm. Then, the fouling potential and reversibility of the different samples (granules, supernatant and raw mixed liquor) were assessed by measuring critical fluxes and through filtration tests. Various hydrodynamic conditions, i.e. gas sparging and recirculation, were applied to evaluate the impact of shear stress on fouling propensity. Results revealed that the supernatant fraction, composed of fine compounds and micro-particles, had a strong fouling potential, whilst the granule fraction led to minor fouling filtration resistance. Three-dimensional excitation emission fluorescence spectroscopy emphasised the prominent role of colloidal proteins in G-AnMBR membrane fouling. During the filtration test of raw mixed liquor, the fouling propensity of the micro-particles was lowered, since the structural cake layer was modified. Gas sparging allowed for the mitigation of cake formation, but excess of shear forces may lead to granule break-up and more irreversible fouling. Liquid recirculation led to a higher filtration resistance, but almost all the membrane permeability was recovered by physical cleaning. A short filtration cycle without gas sparging followed by a short period of relaxation and gas sparging could be a suitable fouling mitigation method. In this way, release of micro-particles from granule break-up could be limited, the cake build-up would be mostly reversible by physical cleaning, and the energy demand of gas sparging would be greatly reduced, thereby improving the energy neutrality of the G-AnMBR biotechnology.

KEYWORDS

membrane; granular sludge; membrane fouling; gas sparging; membrane cleaning.

1. Introduction

The anaerobic membrane bioreactor (AnMBR) is an emergent biotechnology that combines anaerobic digestion and membrane filtration. This hybrid technology is drawing attention for domestic wastewater treatment due to its competitiveness in terms of (i) conversion of organics into methane, (ii) effluent quality and (iii) reactor compactness [1,2]. Many lab- and pilot-scale studies have proven that AnMBR is a sustainable and efficient alternative to conventional energy-intensive processes, which could be suitable for low-energy, water-scarce, low-income and space-limited areas [3,4].

Nonetheless, a major hindrance to AnMBR scale-up and implementation in mainstream wastewater treatment is membrane fouling, as this reduces process productivity and increases energy, operational and maintenance costs (e.g. chemicals, membrane replacement, etc.) [1,5]. Among strategies to reduce AnMBR fouling, the granular-sludge-based anaerobic membrane bioreactor (G-AnMBR) has gained prominence in the last decade, since granules simultaneously boost the biomass activity and reduce membrane fouling [4,6,7]. Granular sludge is characterised by a self-immobilisation of biomass into compact and dense aggregates which form well-established micro-ecosystems. The structural arrangement of the granules imparts high settling capacity, efficient methanogenic activity and high strength to loading rates changes and shocks [2]. Zhang et al. (2021) found that 39.9% of fouling mitigation in a granular membrane bioreactor (MBR) was due to the scouring effect of granules over the membrane surface, while 50.3% was attributed to granule structure [8]. The mechanical scouring effect of the granular material expanded by gas sparging has been reported effective in diminishing membrane fouling in MBR by friction with the membrane and by enhancing the collision between granules and suspended sludge, thus reducing their deposition [8,9]. Due to the higher density of granules, granular sludge is less easily pushed towards the membrane surface than suspended sludge. It is further hypothesised that the large size and solid structure of granular biomass and the immobilisation of extracellular polymeric substances (EPS) within granule structure limit fouling (i.e. pore blocking, deposition and thickness of the cake layer on membrane surface) compared to conventional flocculated sludge MBR [9,10]. Actually, Martin-Garcia et al. (2013) measured a concentration of soluble microbial products (SMP) at least twice as high in a flocculated AnMBR than in a G-AnMBR. Moreover, some solid and colloidal organics are adsorbed and biodegraded inside the granular sludge bed, which is supposed to cause less membrane fouling [11,6]. [12] found that large granules ($d_p \geq 1.2$ mm) and small granules ($d_p \leq 1$ mm) were associated to high flux and low membrane fouling because of loose cake layer structure and less EPS-membrane adhesion, respectively. Conversely, they found that granular sludge with intermediate size ($1 \leq d_p \leq 1.2$ mm) was responsible of more severe fouling due to both compact cake layer and higher adhesion of EPS to membrane surface. Hence, the size of granules has been also identified as a determining factor in the extent of membrane fouling.

The granular sludge matrix is a complex mixture. Based on the size distribution, the granular sludge matrix is generally divided into various fractions, such as (i) granules, (ii) sludge flocs, (iii) micro-particles – including free bacteria and micro-organisms, colloidal and sub-visible particles (0.45 – 15 µm), and (iv) dissolved compounds, e.g. biopolymers, salts and SMP [13,14]. All these fractions could be of influent origin, the result of the bacterial activity, or process dependent and they all might cause membrane fouling [15,14,2]. Several studies have focused on the characterisation of the fouling phenomena in conventional AnMBR. In AnMBR studies, micro-particles were found to dominate the membrane fouling phenomenon [14,15]. Yao et al. (2020) suggested that cake layer formation and biofouling occurred concurrently within the AnMBR, since analogous organics and micro-organisms were found in micro-particle fraction and foulant components. Subsequently, even though granular sludge partly helps membrane fouling mitigation compared to conventional flocculated sludge, fouling concerns remain and need to be better understood to define effective fouling mitigation and cleaning strategies.

Based on the most common MBR fouling mitigation strategy, some studies have investigated different permeate fluxes (from 5 to 20 $L.m^{-2}.h^{-1}$ (LMH)) and specific gas demand (SGD) (0.1 – 2.0 $m^3.m^{-2}.h^{-1}$) to identify the best operating and hydrodynamic conditions for G-AnMBR to maintain high membrane permeability with low energy requirements and treatment costs [16,17]. Vinardell et al. (2022) stated that operating at moderate fluxes and gas sparging rates (J_{20} = 7.8 LMH; SGD = 0.5 $m^3.m^{-2}.h^{-1}$) could be the most favourable membrane fouling control strategy in G-AnMBR and balance process productivity and process economics. Wang et al. (2018a) tested continuous and intermittent gas sparging regimes and filtration cycles and stated that shear rate, gas sparging frequency and filtration cycle length are of high importance for delivering sustained membrane filtration. Intermittent filtration associated with intermittent gas sparging has been identified as the best fouling mitigation method in G-AnMBR, since low residual fouling resistance and energy neutrality can be achieved [17]. However, the authors suggested further investigations to properly manage operating conditions.

To implement suitable and affordable fouling management, it is essential to understand the inherent G-AnMBR fouling phenomenon, since membrane fouling characteristics are matrix-dependent. To the best of the authors' knowledge, no previous studies have explicitly explored the fouling potential of an anaerobic granular sludge matrix. The aim of this study is therefore to reveal the fouling potential and mechanisms of an anaerobic granular sludge. To provide an in-depth assessment, the G-AnMBR mixed liquor was fractionated by sieving into two parts, the granules fraction and the supernatant fraction. The threshold size that distinguishes a granule from a flocculated sludge varies from 0.1 mm to 1 mm, depending on the study [18–20]. In this study, bioparticles above 0.125 mm were regarded as granules. Filtration tests were conducted on the raw granular mixed liquor, the granules fraction and the supernatant fraction to evaluate their impact on membrane fouling. Since hydrodynamic conditions and the resulting shear stress are a key driver in membrane fouling mitigation, two gas sparging conditions and a liquid recirculation condition were tested in each filtration test. The critical flux concept and resistance-in-series model were used to determine fouling rate and reversibility of each fraction for the three different hydrodynamic conditions. Three-dimensional excitation/emission fluorescence analyses were conducted to characterise the foulants.

Specific objectives are to (i) make a direct and systematic comparison of the fouling behaviour of the different fractions, (ii) determine the main compounds responsible for membrane fouling, (iii) find out the possible interactions between granules and supernatant fractions and their effect on fouling, and (iv) identify the impact of the hydrodynamic conditions on the granular sludge and fouling behaviour to increase understanding and help decision making about fouling strategies.

2. Materials and methods

2.1 Anaerobic granular sludge fractions

Raw granular anaerobic sludge (called the "raw mixed liquor") was taken from a mesophilic (35-38°C) industrial Upflow Anaerobic Sludge Blanket (UASB) reactor treating the process water from the manufacturing of recycled paper (Saica Paper Champblain-Laveyron, France). Four litres of raw mixed liquor at a constant total suspended solids (TSS) concentration of 10 g/L were split through a standard sieve of 0.125 mm mesh size. Granules retained on the sieve ($d_p \geq 0.125$) were resuspended into four litres of deionised water and represent the granules fraction from now on. The four litres of liquid and particles that flowed through the sieve were regarded as the supernatant fraction ($d_p < 0.125$). Fouling propensities of (i) granules, (ii) supernatant, and (iii) raw mixed liquor were systematically assessed.

2.2 Experimental set-up

The experimental lab-scale system, shown in Fig. 1, was composed of two sections with an effective volume of 4 L. The lower part of the reactor consisted of a thin parallelepiped-shaped zone (215 x 24 x 405 mm) where the membrane cartridge was immersed and the upper part was a flared section. The bottom of the reactor included both a liquid recirculation and an aeration diffuser used separately according to the operating conditions applied. The liquid recirculation was carried out by a peristaltic pump (Watson Marlow (WMFTG), UK). Supernatant was pumped from the top of the reactor and reintroduced under the membrane through a 10 mm hole placed in the middle of the section. The gas sparging was done by a hollow tube with three drilled holes (1 mm diameter) distributed along the length and controlled by a gas flowmeter. The microfiltration membrane used was a flat sheet module from KUBOTA Membrane Europe (UK) in Polyethylene Terephthalate (PET) and Chlorinated Polyethylene (PE-C) with a nominal pore size of 0.4 μm, 0.11 m² surface area and 6 mm cartridge width. The permeate was suctioned through a peristaltic pump (Watson Marlow (WMFTG), UK) and returned to the reactor to maintain a constant volume. The transmembrane pressure (TMP) was obtained through a pressure gauge installed on the permeate line. The water temperature (T) in the reactor was monitored. Pressure and temperature data were recorded using a Bluetooth-based system provided by Instrument Works (Waterloo, Australia). Visualisation, acquisition and storage of all data was realised thanks to the Dataworks software (Instrument Works, Waterloo, Australia). Membrane flux (J_T) was set at 20 $L.m^{-2}.h^{-1}$ (LMH) and the corresponding normalised flux at 20°C (J_{20}) was recalculated using Equation (1).

$$J_{20} = \frac{J_T . \mu_T}{\mu_{20}} \quad (1)$$

where J_{20} is the normalised flux at 20°C ($m^3.m^{-2}.s^{-1}$) and μ_{20} and μ_T (in Pa.s) are the viscosity of water at 20°C and at the working temperature T (°C) respectively.

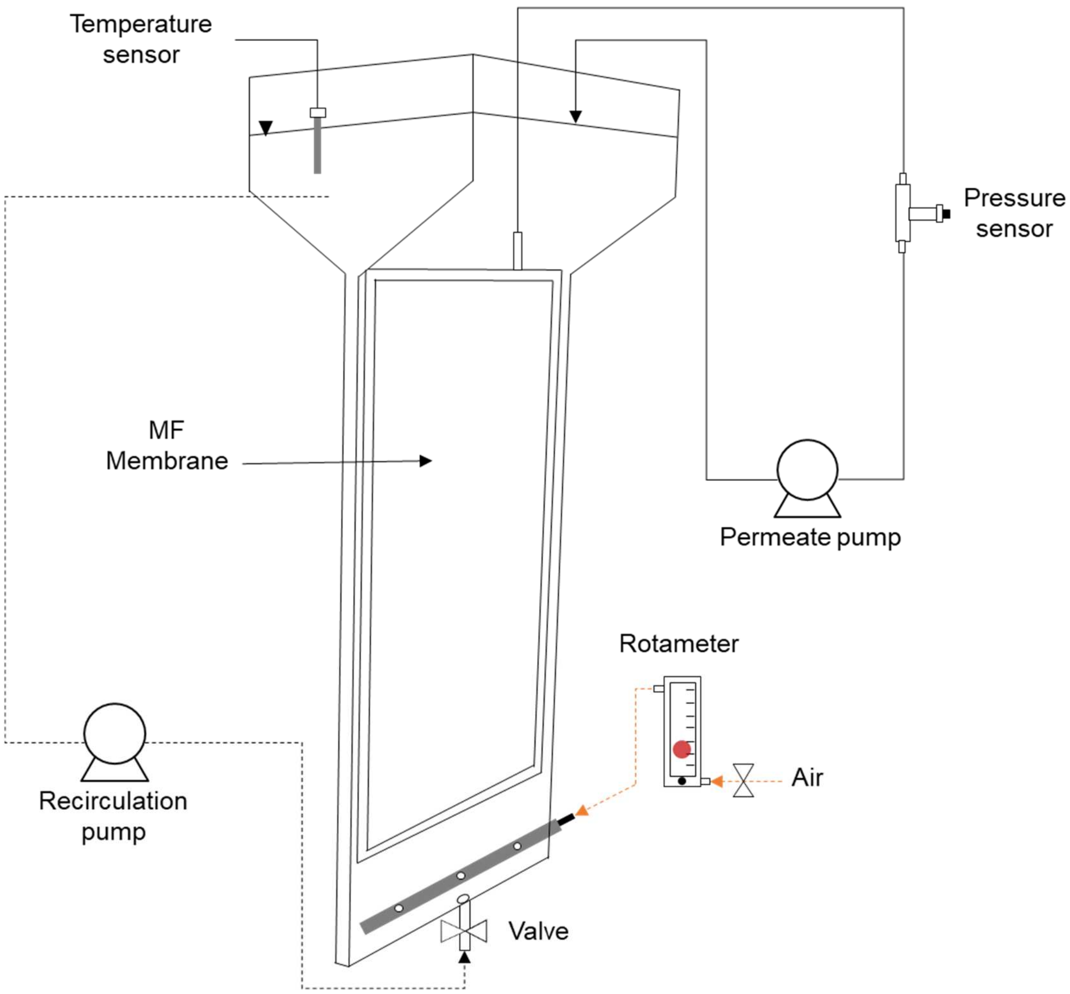

Fig. 1 – Schematic representation of the experimental set-up

2.3 Filtration tests

Filtrations tests were conducted for the three sludge fractions (raw mixed liquor, granules and supernatant). Each experiment consisted of filtration tests based on five consecutive operating cycles composed of 45 min of filtration and 90 s of relaxation. Three hydrodynamic conditions were investigated with the aim of evaluating the influence of turbulence on filtration performances. Hence, a liquid recirculation of 24 L/h (RE) and two aeration flow rates of 25 L/h (A25) and 100 L/h (A100) were applied resulting in shear stress of 15, 205 and 409 s^{-1} respectively (see equations in supplementary data). For RE, the crossflow velocity was about 11 m/h and the specific gas demand was 0.23 and 0.91 $m^3.m^{-2}.h^{-1}$ for A25 and A100, respectively. Before each filtration test, the permeability of the clean membrane was measured with deionised water through flux-stepping increments and determined as follows:

$$J_{20} = Lp.TMP \tag{5}$$

where Lp is the permeability ($L.m^{-2}.h^{-1}.bar^{-1}$), J_{20} is the normalised flux at 20°C ($L.m^{-2}.h^{-1}$) and TMP is the transmembrane pressure (bar).

2.4 Critical flux

Critical fluxes (J_c), corresponding to the onset of prominent fouling, were assessed by the flux-step method [21] for each fraction and hydrodynamic condition tested. The permeation rate was increased stepwise from 2 LMH to 30 LMH and then incrementally decreased. The corresponding TMP was continually recorded. The step duration was fixed at 10 minutes and a step height of 2 LMH and 4 LMH was chosen for the ascending and descending phases, respectively. Le Clech et al. (2003) established three key TMP-based parameters to determine the critical flux, namely: (i) the initial TMP increase (ΔP_n), (ii) the TMP increase rate $(dTMP/dt)_n$, and (iii) the average TMP $(P_{average})_n$. All these parameters are depicted below:

$$\Delta P_n = TMP_i^n - TMP_f^{n-1} \tag{2}$$

$$\left({}^{dTMP}/_{dt}\right)_n = \frac{(TMP_f^n - TMP_i^n)}{t_f^n - t_i^n} \tag{3}$$

$$P_{average_n} = \frac{TMP_i^n + TMP_f^n}{2} \tag{4}$$

where TMP_i^n and TMP_f^n are the initial and final TMP, respectively, of the n flux step, t_i^n is the starting time and t_f^n is the ending time of this step.

The three parameters were calculated for each flux step. When the TMP-based parameters were no longer constant between flux steps and deviated from clean water values, the critical flux was considered to have been reached. The critical flux values given in this study are the average of the critical flux obtained through each parameter. Hence, the critical flux mentioned in this study is not in its zero-rate strict form, but corresponds to the flux level under which a sustainable filtration can be achieved.

2.5 Fouling propensity and fouling reversibility

Filtration resistances were determined following Darcy's law (Equation (6)).

$$R_t = \frac{TMP}{\mu_{20} \cdot J_{20}} \tag{6}$$

where R_t is the resistance (m^{-1}) and TMP is the transmembrane pressure (Pa).

Membrane fouling was characterised by means of the resistance-in-series model. In this study, the total resistance (R_t) is defined as the sum of the intrinsic membrane resistance (R_m) and the fouling resistance (R_f) which, in turn, was divided into the resistances caused by reversible fouling, irreversible fouling and residual fouling ($R_{reversible}$, $R_{irreversible}$, $R_{residual}$ respectively) as described in Equation (7) and (8).

$$R_t = R_m + R_f \tag{7}$$

$$R_f = R_{reversible} + R_{irreversible} + R_{residual} \tag{8}$$

The above-mentioned resistances were determined by filtering deionised water in the same hydrodynamic conditions as the filtration tests, using the following experimental procedure: (i) R_m was measured by filtering deionised water through the clean membrane; (ii) R_t was evaluated using the fouled membrane at the end of the filtration test; (iii) R_f was deduced from Equation (7); (iv) superficial cleaning with water was undertaken, taking the fouled membrane out of the reactor and flushing the surface with 1 litre of deionised water, after which the remaining resistances ($R_{irreversible} + R_{residual}$)

were measured by filtering deionised water; $R_{reversible}$ was then calculated using Equation (8); finally, (v) a two-hour chemical cleaning by soaking in a 0.2% sodium hypochlorite solution was carried out under aeration, and the leftover resistance $R_{residual}$ was measured; $R_{irreversible}$ was then deducted from Equation (8).

2.6 Analytical methods

2.6.1 Particle size distribution

Particle size distribution (PSD) was performed on the raw mixed liquor before and after filtration tests at A25, A100 and RE. Size fractionation was done by wet sieving. The standard sieves used were of 1.0, 0.63 and 0.125 mm mesh sizes, resulting in four fractions: large granules ($d_{p \geq 1}$), medium granules ($d_{p\ 1\text{-}0.63}$), small granules ($d_{p\ 0.63\text{-}0.125}$), and flocs and fines ($d_{p\ <\ 0.125}$). Total solids of each fraction were measured according to Standard methods [22]. The PSD was expressed as a fraction's mass distribution [2].

2.6.2 Three-dimensional excitation emission matrix fluorescence

Three-dimensional Excitation Emission Matrix (3DEEM) fluorescence was used to characterise and semi-quantify the dissolved and colloidal organic matter (DCOM), as 3DEEM samples were filtered at 0.45 µm. The cleaning water from the physical cleaning and the raw mixed liquor before and after filtration tests were analysed. Three-dimensional excitation emission matrices were obtained using a Perkin-Elmer FL6500 spectrometer (USA). Excitation and emission scan ranges were fixed at 200-500 nm and 280-600 nm, respectively, while scan speed was set at 12,000 nm/min, incremented to 10 nm. The slit width was 5 nm for both excitation and emission. Every sample was associated with a Milli-Q water blank analysed in the same conditions. To circumvent the over-quantification caused by Raman and Rayleigh water scatter peaks, all spectra were scatter-corrected by the blank sample [23]. From the 3DEEM spectra, four regions were distinguished, based on their specific fluorophores [24]. Region I+II was associated with protein-*like* fluorophores (tyrosine) ranging from λ_{ex} = 200-250nm to λ_{em} = 280-380nm, Region III (λ_{ex} = 200-250nm / λ_{em} = 380-600nm) corresponded to fulvic acid-*like* molecules, Region IV (λ_{ex} = 250-350nm / λ_{em} = 280-380nm) was associated with soluble microbial product (SMP)-*like* molecules (Tryptophan), and Region V (λ_{ex} = 250-500nm / λ_{em} = 380-600nm) corresponded to humic acid-*like* molecules. Region III and IV were merged into a single region III+IV, called humic substances. The normalised volume of fluorescence (in arbitrary unit per nm^2 ($A.U/nm^2$)) beneath each area was calculated as a function of the fluorescence intensity at each excitation-emission pair.

2.6.3 Proteins and polysaccharides

Protein (PN) and polysaccharide (PS) contents were used to characterise the different fractions and to follow any modification or release of these organic compounds during the experiments. The colorimetric Lowry and Dubois methods were used for PN and PS, respectively [25,26]. Bovine Serum Albumin (BSA) and glucose were used as calibration solutions. All samples were pre-filtered through a 0.45 µm acetate cellulose filter before dosing.

3. Results and discussion

3.1 Granular sludge characteristics' behaviour during the filtration test

In order to follow the raw mixed liquor trends during the filtration test, particle size distribution (Fig. 2a), total volume of fluorescence (Fig. 2b), and PS and PN concentrations (Fig. 2c) were measured. The initial raw mixed liquor was mainly composed of large granules, i.e. around 95% of mass fraction of particles over 0.125 mm in diameter ($d_{p\ \geq\ 0.125}$). Initially, the DCOM of the raw mixed liquor was predominantly composed of proteins (54.2 ± 4.0 %) and humic substances

(40.9 ± 5.0 %) and with a total volume of fluorescence of 3.6 ± 0.5 10^{10} A.U.nm^{-2}. The recirculation (RE) condition had a slight effect on the PSD with a lower proportion of smaller compounds, probably due to the aggregation of particles resulting from the low shear rate, however, no significant change in organic composition was observed. In contrast, in the A25 and A100 conditions, the large granule content ($d_{p \geq 1.0}$) decreased from 88% to 83% and 77%, respectively, showing that higher shear stress increased the number of smaller granules. In the same way, the volume of fluorescence reached 4.9 ± 0.5 10^{10} and 5.6 ± 0.3 10^{10} A.U/nm² for A25 and A100, respectively, that is, +40% and +58% more than the initial value. Similarly, the concentration of PN increased especially for both aeration rates A25 and A100 (+67% and +129%, respectively) confirming the release of protein substrates from the granules. The greater the forces of attrition, the higher the total volume of fluorescence and proteins became, underlining granule degradation and its release of fines and DCOM. This confirmed the pre-established positive correlation between hydrodynamic forces, attrition forces and granule disruption. Granule attrition created crevices on the granule surface and pushed surface bacteria and DCOM off the granule [27]. Moreover, soluble COD (sCOD) membrane removals are shown in supplementary materials. The sCOD removal rate was globally not affected by the hydrodynamic conditions, as the sCOD rejection was constant and about 27.2 ± 10.5 %.

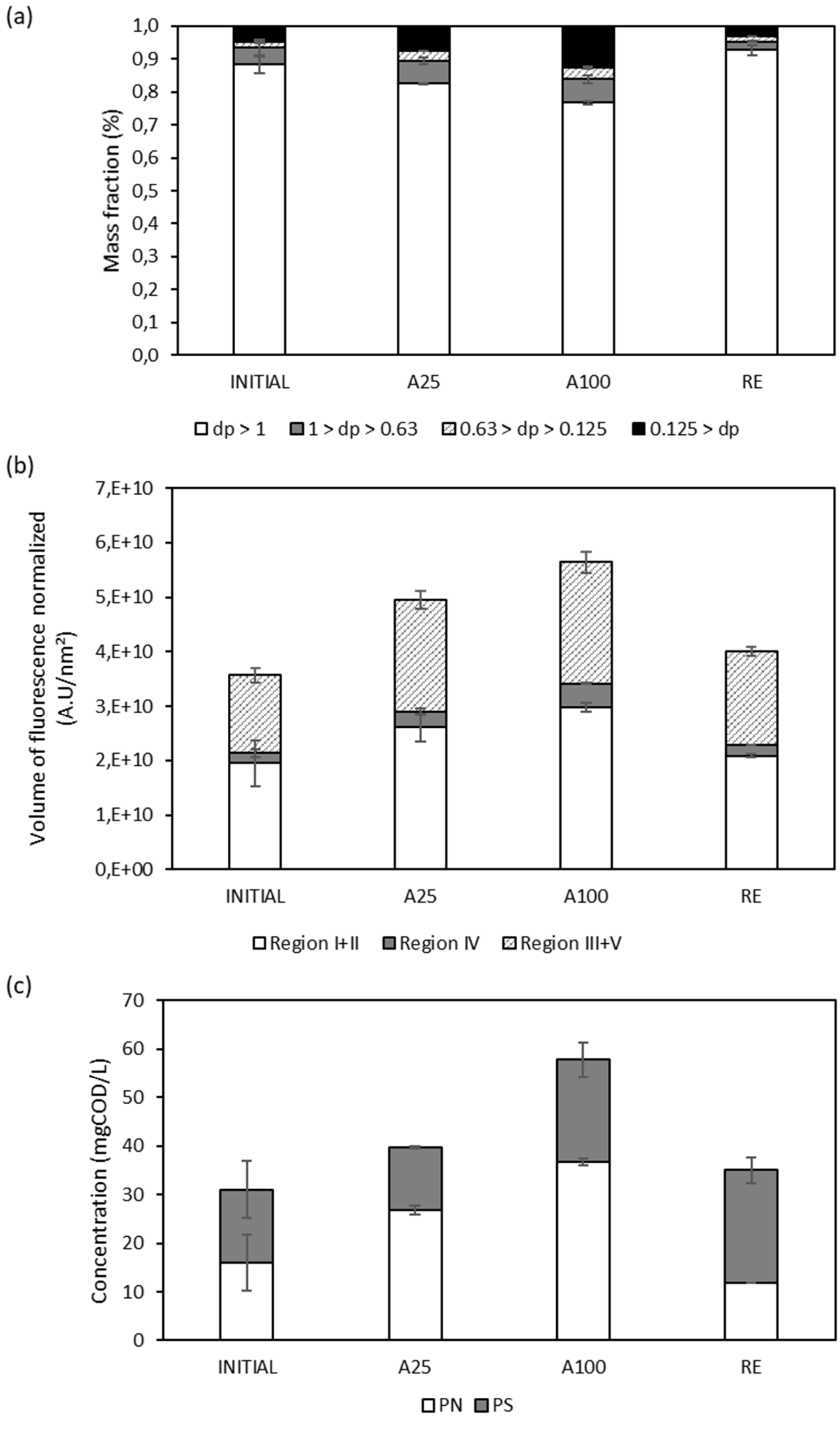

Fig. 2 - Evolution of (a) Particle Size Distribution (PSD), (b) relative percentage volume of fluorescence from 3DEEM and (c) concentration of PN and PS of the raw mixed liquor before the experiment (initial) and after each hydrodynamic operating condition applied (A25, A100, RE).

3.2 Effect of sludge fraction and operating conditions on critical flux

The critical flux results are given in Fig. 3. In all conditions, the granule fraction showed lower fouling potential, with the lowest TMP in all conditions applied, which resulted in highest critical flux values (J_c > 22 LMH) (Fig. 3d). The TMP profiles also showed that no incremental effect occurred when the supernatant and granules were both present in the raw mixed liquor. Hence, the supernatant was found to be the major foulant, emphasised by the lower and similar critical fluxes of both the raw mixed liquor and supernatant fractions. These results support those observed in recent studies which stated that micro-particles (0.45-10μm) – including some colloids – were mainly responsible for membrane fouling in AnMBR [13,14,28].

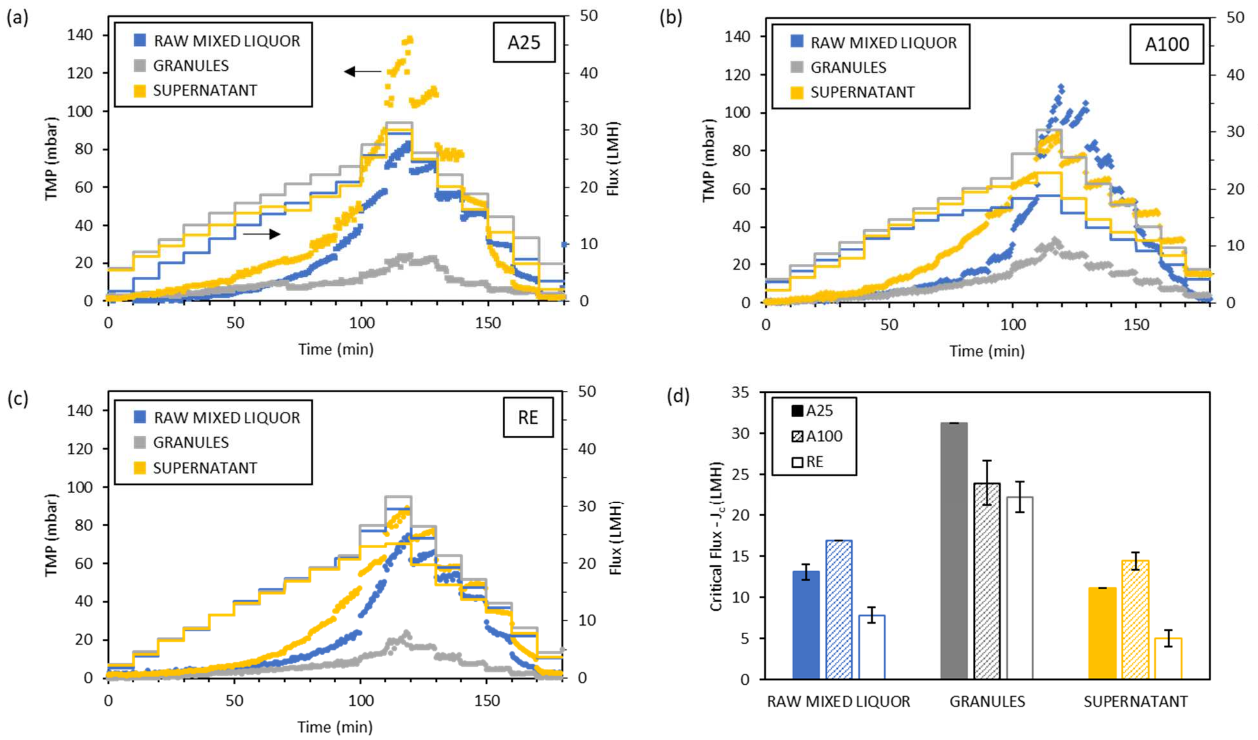

Fig. 3 – Evolution of TMP and flux for the raw mixed liquor and the two fractions at the different operating conditions (a) A25, (b) A100, (c) RE and the (d) critical flux obtained through the TMP-based indicators.

The increase in hydrodynamic conditions, induced by gas sparging, had a beneficial effect on filtration performance, since the critical flux values were positively related to the shear stress, except for the granule fraction (Fig. 3d). In the latter case, hydrodynamic conditions were too high and detrimental for the granule filtration capacity with a drop in critical flux from 31.3 LMH in A25 condition to 24 LMH for A100. This phenomenon can be linked to the granule disruption mentioned earlier which led to a rise of fine particles and colloidal and dissolved compounds (Fig. 2). These findings support that shear forces are of high importance in mitigating membrane fouling but the use of gas scouring as a fouling mitigation method has to be precisely adapted to avoid the detrimental effect of the shear stress, such as granular biomass disruption, membrane fouling by fines, and energy overspending.

In addition, while comparing the TMP reached during the flux increasing phase and decreasing phase, several phenomena were observed. An apparent hysteresis was observed, for the supernatant fraction and raw mixed liquor especially, suggesting non-reversible fouling by the tested turbulence (see supplementary data). Interestingly, below the critical flux, the gap between the ascending TMP and the descending TMP was reduced in conditions A25 and A100. This phenomenon highlights that above the critical flux, there was still an accumulation of foulant on the membrane surface. Conversely, below the critical flux, no significant deposition of particles occurred, so during the decreasing phase, the TMP declined because of the flux reduction and the cake layer detachment under the aeration effects. Nevertheless, the granule fractions showed no apparent hysteresis under both aeration conditions, meaning that particle deposition was mostly reversible regardless of flux. Finally, in the RE condition, a strong level of hysteresis was observed for all fractions. During the decreasing flux steps, the TMP dropped linearly, which emphasised the absence of additional accumulation and a lack of foulant detachment [29].

3.3 Membrane filtration behaviour

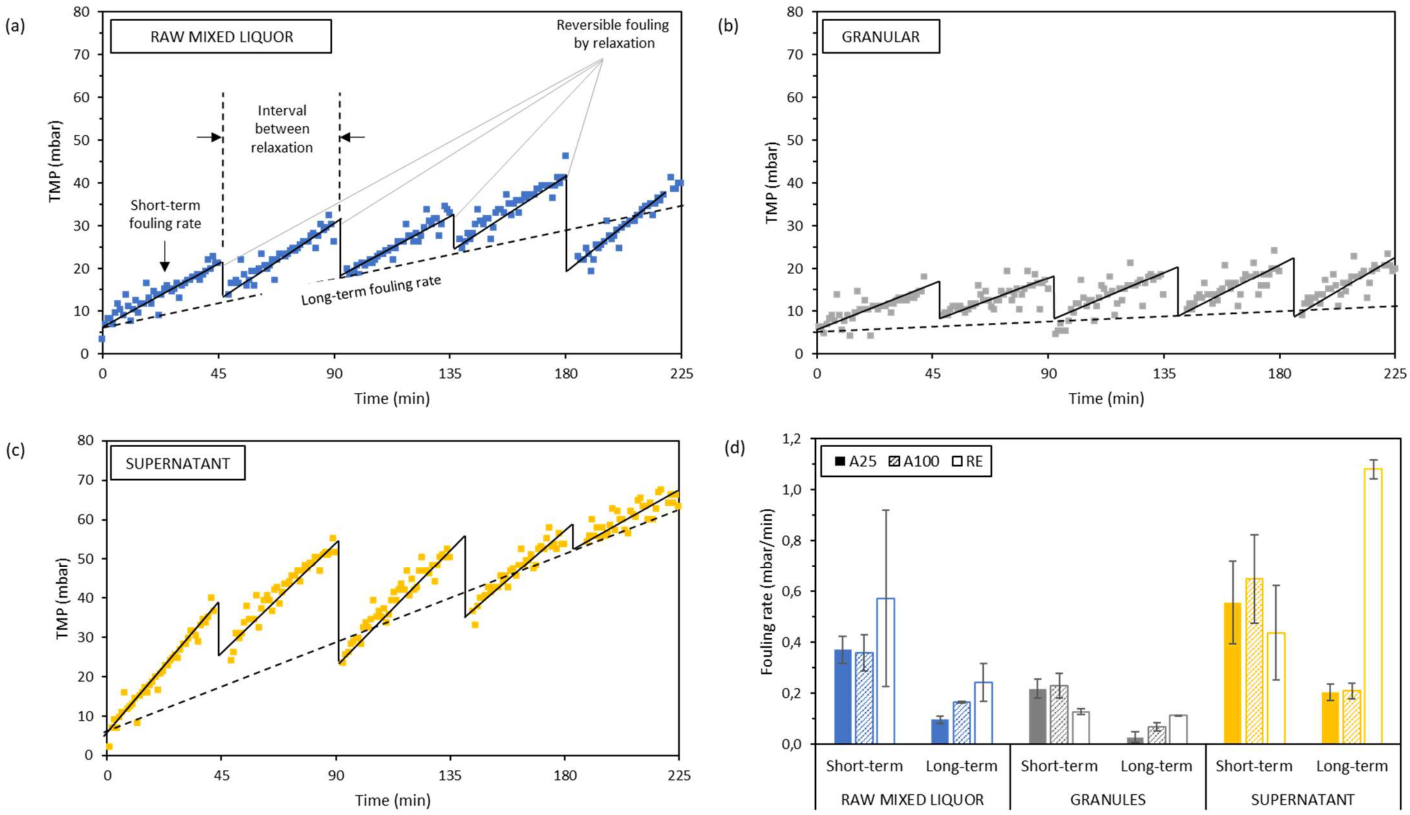

Fig. 4 – Evolution of the TMP over time during the five cycles of filtration with aeration at 25L/min for (a) the raw mixed liquor, (b) granules,(c) supernatant and (d) the corresponding average reversible fouling rate for each filtration condition (A25, A100, RE) and for raw mixed liquor and the two fractions.

The change in TMP during the filtration tests of raw mixed liquor and the two fractions for the A25 condition are presented in Fig. 4. An overview of the A100 and RE conditions is provided in the supplementary data. From these TMP profiles, two fouling rates were determined: (i) the average short-term fouling rate, which corresponds to the mean fouling rate observed between intermittent relaxation steps and (ii) the long-term fouling rate (Fig. 4a and Fig. 4d). First, the lowest fouling capacities of the granule fraction were confirmed, whatever the hydrodynamic conditions, with a negligible TMP increment (~0.1-0.2 $mbar.min^{-1}$) during operation cycles. In comparison, the supernatant presented a TMP increase almost three times higher (~0.45-0.65 $mbar.min^{-1}$), highlighting its stronger fouling propensity. This is in accordance with previous results which stated that the membrane permeability declines with the decrease of the particle size deposition which forms a more compact fouling deposit and leads to higher pore blocking [8,30]. Interestingly, under aeration conditions (A25 and A100), the raw mixed liquor sample, which combines granules and supernatant fractions, exhibited TMP profiles and fouling rates below the supernatant ones, with a short-term fouling rate around 0.35 $mbar.min^{-1}$, confirming the benefit effect of granules upon the supernatant fouling behaviour. Indeed, it has been reported that the granular sludge structure is largely favourable for membrane mitigation due to the larger particle diameter than membrane pore, leading to low pore blocking. Moreover, when combined with gas sparging, the granules had an additional scouring effect, which helped to diminish the flocs accumulation on the membrane surface and decrease the penetration driving force of fine particles on membrane pores [8].

With regards to the hydrodynamic conditions applied, no significant differences were observed for short-term fouling rates between the A25 and A100 conditions, regardless of the fraction filtered. Numerous studies have shown that there is a critical gas velocity above which the gas sparging flow rate no longer impacts the fouling rate [11,17,31]. Above the threshold gas sparging rate, the increase of shear stresses has no additional effect on particle deposition mitigation and the coalescence of the air bubbles can even reduce the shear events in the vicinity of the membrane [32]. Furthermore, the back-transport resulting from the hydrodynamic conditions has been positively correlated to the particle size, meaning that smaller particles face lower shear-induced diffusion

[33,34]. Hence, it is likely that membrane fouling in G-AnMBR is mainly a result of smaller compounds and dissolved matter.

Moreover, the long-term fouling rate values (Fig. 4d) for the A100 condition were found to be higher than the A25 for the granules and raw mixed liquor (0.07 vs 0.03 $mbar.min^{-1}$ and 0.16 vs 0.10 $mbar.min^{-1}$ respectively). This phenomenon is almost certainly due to the attrition of the granules that increased the amount of smaller compounds (see Fig. 2a), as well as extracellular polymeric substances [31], which might contribute to membrane fouling that is less responsive to the relaxation step. Moreover, for the granule fraction with RE condition, the short-term and long-term fouling rates were almost similar, suggesting that the relaxation steps did not have a significant fouling mitigation effect. Conversely, the RE condition is the least effective solution for fouling management when fine compounds ($d_{p < 0.125}$) are in abundance (i.e. raw and supernatant samples), probably due to a lack of shear events at the water-membrane interface. These filtration tests support the careful consideration that should be given to the hydrodynamic parameters in G-AnMBR. Shear conditions have to be great enough to prevent membrane fouling and provide a long-lasting filtration, but not too high to avoid excessive energy consumption and adverse effects on granular biomass. This is of great importance, because the damage of granular sludge does not only have a detrimental effect on membrane fouling, but it also reduces the organic removal efficiency, since biomass activity and syntrophic associations are hindered [4,35].

3.4 Filtration resistance

Fig. 5 shows the filtration resistances measured at the successive stages of the filtration tests and the different types of fouling deducted from the resistance-in-series. A significant difference was observed between the resistance recorded at the end of the filtration test and the total resistance measured on the fouled membrane by filtering deionised water, notably for the A25 and A100 conditions. Therefore, the average total resistances measured during the 10 last minutes of fifth filtration cycle are also presented in Fig. 5. This difference may be due to the concentration polarisation occurring during the filtration of fractions but mainly to the manipulation of the membrane and aeration shear stresses during the permeability measurement, which unintentionally contributed to removing the fouling during the total resistance measurement. In fact, it is as if a membrane cleaning by gas sparging had been performed. Nonetheless, these facts show that the filtration resistances caused by cake build-up were easily suppressed by gas sparging and, therefore, counted as reversible fouling.

The higher fouling potential of the supernatant fraction and the synergetic effect between granules and supernatant fractions were confirmed by the total resistance, measured at the end of the fifth filtration cycle, which diminished from 14.2 10^{11} m^{-1} for supernatant filtration to 7.5 10^{11} m^{-1} for raw mixed liquor in A25 condition, from 13.6 10^{11} to 8.5 10^{11} m^{-1} at A100, and from 60.7 10^{11} to 33.3 10^{11} m^{-1} at RE. In the presence of granular sludge, it has been reported that the cake layer built on the membrane surface had a lower filtration resistance by means of a high cake porosity and the collision of granules with flocs, biopolymers and membrane surface (Zhang et al., 2020; Zhang et al.,2021). These results clearly show that the lack of shear stress in the vicinity of the membrane (e.g. RE condition) led to a stronger increase in fouling resistance, since the applied shear forces were not sufficient to counteract the penetration driving forces [8] and to promote the scouring effect of the granules. It should be noticed that in the RE condition, constant filtration fluxes were difficult to sustain and thus high resistance variabilities were observed in the experiment (see supplementary material).

Fig. 5d describes the relative reversibility of the fouling deposit for each experiment. In any hydrodynamic condition, the filtration resistance built up during the filtration of the supernatant was predominantly reversible (≥ 98%), meaning that almost all of the fouling was removed by the physical cleaning. Interestingly, for the granule fraction, in both aeration conditions, around 20% of the total resistance remained after superficial cleaning ($R_{irreversible}$ + $R_{irrecoverable}$), and 7% of the filtration resistance was not even recovered after chemical cleaning ($R_{irrecoverable}$). Regarding the raw mixed liquor, about 10% of the fouling resistance remained after physical cleaning. Based on these findings, it could be suggested that different fouling mechanisms were implicated relative to the fraction filtered. During the filtration of the supernatant fraction, the rapid accumulation of micro-particles and fines led to the build-up of a cake layer. Then, under the continuous filtration, the cake layer was compressed, causing the change in cake structure and a shift in particle size distribution to a larger size next to the membrane surface [36]. The cake consolidation allowed for an easier and effective cake removal, since it allows the detachment of large agglomerates and large layer fragments [37]. In contrast, when the supernatant was combined with the granule fraction (i.e. raw mixed liquor), the cake layer was more porous because of larger particle size, which was beneficial for the filtration performance. However, soluble and smallest substances can pass through the loose cake layer and attach to the membrane surface or block the membrane pores [10]. A lower reversibility of small and single particles which interact with the membrane surface has been reported [37] which could explain the measured irreversible and residual resistances.

These distributions of the nature of the fouling should be interpreted with caution, because although it describes the relative repartition of the resistances, it does not highlight their effective resistance to the filtration. Hence, even if a part of the fouling caused by granules (i.e. raw and granule fractions) was not removed by the cleaning methods employed, the filtration resistance caused by the persistent foulants was still low compared to the initial filtration resistance ($R_m = 16.5 \pm 1.1\ 10^{10}\ m^{-1}$).

In contrast, for all fractions in the RE conditions, the initial resistance was restored almost entirely with the physical cleaning (≥ 96%). In this case, the low hydrodynamic conditions resulted in a barely fixed granular sludge bed, so that the granule fraction was not in the vicinity of the membrane and did not take part of the cake layer formation. Therefore, the membrane fouling that took place during the raw and granule fractions must have been composed of micro-particles and non-settable compounds similar to the supernatant fraction and thus had the same compact structure which induced the same degree of reversibility.

Based on these results, a combine fouling mitigation method can be suggested with short intermittent cycles composed of filtration without gas sparging intersected by relaxation and gas sparging periods. In this way, the granules would not be degraded, the fouling deposition would be mostly reversible and the gas sparging energy demand would be lowered. This is in accordance with a previous G-AnMBR study in which, in absence of gas sparging, high fouling resistance was observed, but almost all the accumulated cake was removed by simultaneous use of relaxation and gas sparging [17].

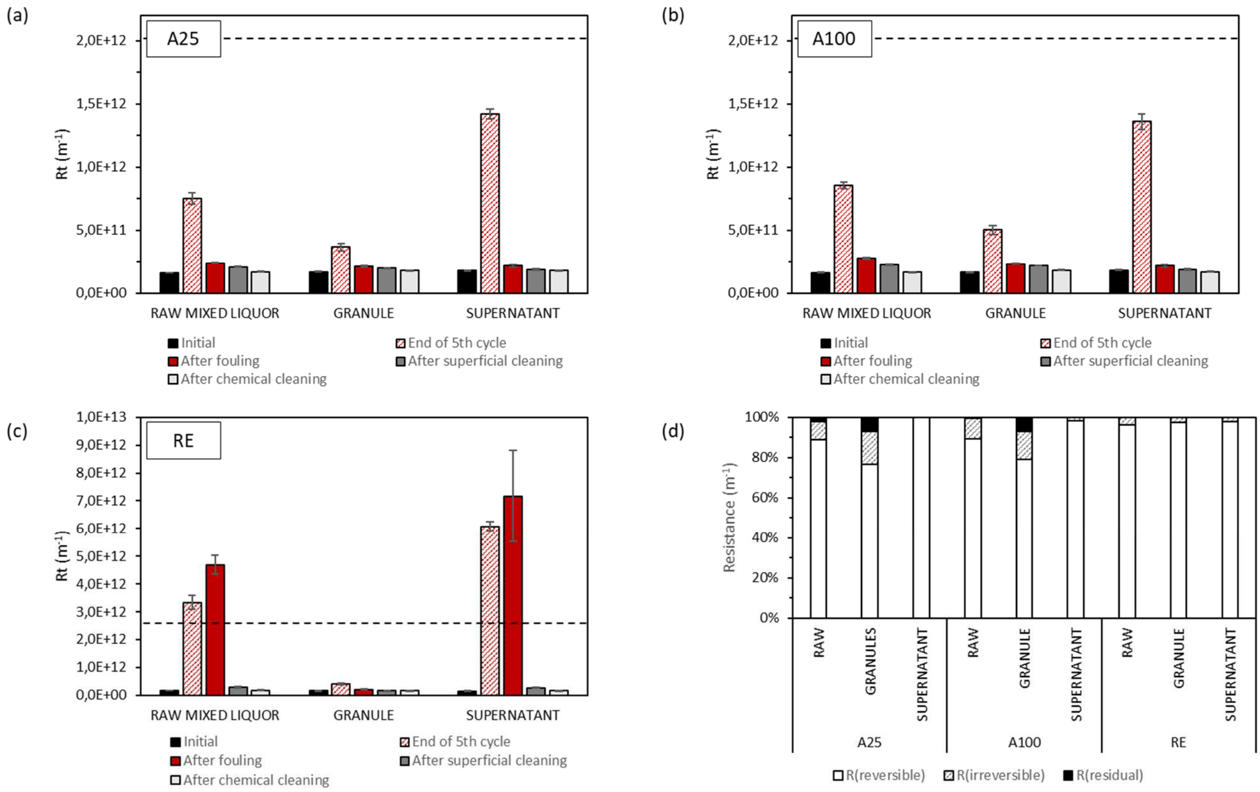

Fig. 5 – Evolution of the filtration resistance at different operating stages: (i) the initial stage (i.e. $R_t = R_m$), (ii) the end of the fifth cycle of filtration, (iii) the fouled membrane, (iv) after the superficial cleaning, and (v) after the chemical cleaning for (a) the 25L/min aeration rate, (b) the 100 L/min aeration rate, (c) the recirculation, and (d) repartition of the different type of fouling resistance for raw mixed liquor and the two fractions at different operating conditions.

3.5 Membrane fouling characteristics

Table 1 presents the repartition of the volume of fluorescence obtained through 3DEEM for rinsing water collected from each superficial cleaning – i.e. the reversible foulant. In all cases, the largest amount of fluorescence appeared in region I+II, accounting for 68-85% of the total fluorescence. According to Jacquin et al. (2017), region I+II from the 3DEEM fluorescence is associated with colloidal proteins and, consistent with the present results, they appeared to be the major foulants in G-AnMBR . It appears that micro-particles (0.45-10 µm) play a key role in G-AnMBR, as already observed in classical AnMBR studies [14], and organic foulant compounds are mainly protein-*like* substances [38]. The critical role of proteins has already been underlined due to their greater hydrophobicity, which induces a higher adhesion capacity of protein-rich compounds to the polymeric membrane surface [17,39]. The total volume of fluorescence of every fraction in RE conditions was definitely higher than under aeration conditions. It seems that the higher filtration resistance is due to a larger amount of foulants on the membrane surface rather than a different and harsher type of foulant. Moreover, the volume of fluorescence increased in the A100 condition relative to A25 which described a stronger organic matter deposition, certainly linked to the granule disruption and protein release mentioned previously (see Section 3.1).

4. Conclusion

From the present study, the following conclusions can be drawn:

- Granules ($d_{p \geq 0.125}$) had a negligible fouling potential with a fouling rate below 0.2 mbar.min^{-1} whatever the hydrodynamic conditions used.
- The supernatant fraction, composed of fine compounds and flocs ($d_{p < 0.125}$), was the key driver of membrane fouling in G-AnMBR. Nevertheless, the related membrane fouling was reversible with more than 98% of the fouling resistance recovered by simple water cleaning. Moreover, the compression of the cake layer under the drag forces led to a denser layer, which enables its complete removal.
- In the raw mixed liquor, where supernatant and granules are mixed, the fouling rate was lower compared to the supernatant fraction. It is suggested that granules diminished the impact of the fines and micro-particles over membrane permeability through mechanical scouring action and the formation of a more porous and loose cake layer structure. Interestingly, around 20% of the total fouling resistance remained after the superficial cleaning, suggesting that the

loose cake layer does not prevent small and adherent foulants from entering the membrane pore, causing residual fouling.

- Based on the 3DEEM analysis, at least 68% of the fluorescent organic matter from the reversible fouling came from the protein-*like* region regardless of the fraction. Hence, colloidal proteins seemed to be the main organic foulant in G-AnMBR.
- Hydrodynamic conditions were of high importance in mitigating membrane fouling. In tested conditions, gas sparging was more efficient in limiting membrane fouling than recirculation. However, a plateau was reached in gas sparging rate, above which the increase gas flow does not lead to a decrease in fouling rate. Moreover, higher shear stress led to stronger granule disruption, releasing smaller compounds which in turn increased membrane fouling.

Based on the results, it is evident that well-shaped and high-strength granules have to be privileged in G-AnMBR. The induced shear forces have to be sufficient to scour the membrane surface whilst not damaging the granular biomass, nor incurring unnecessary energy consumption. The fouling mitigation-energy nexus could lie at an intermittent filtration cycle associated with the threshold sparging rate. Further investigation and technical-economic analysis have to be conducted to define the most favourable filtration cycle which maximises the net energy balance of the G-AnMBR process. In addition, long-term experiments need to be studied to see the potential composition change of the mixed liquor and fractions over time, and its consequences on fouling behaviour.

Acknowledgements

Gaetan Blandin received the support of a fellowship from the “la Caixa” Foundation (ID 100010434). The fellowship code is LCF/BQ/PR21/11840009.

This work was supported by a grant overseen by the French National Research Agency (ANR) as part of the “JCJC” Programme BàMAn (ANR-18-CE04-0001-01).

Table 1 – Repartition of the volume of fluorescence within 3DEEM regions of the superficial cleaning for the three fractions and hydrodynamics conditions studied.

		RAW MIXED LIQUOR			GRANULES			SUPERNATANT		
Region	Units	A25	A100	RE	A25	A100	RE	A25	A100	RE
I+II	$\times 10^9$ (A.U.$m^{-2}.L^{-1}$)	2,0 (82.1%)	3,0 (84.8%)	18,3 (81.3%)	1,2 (68.0%)	2,3 (78.4%)	8,3 (78.6%)	1,7 (81.7%)	2,8 (76.0%)	18,0 (85.0%)
IV	$\times 10^9$ (A.U.$m^{-2}.L^{-1}$)	0,1 (4.6%)	0,2 (4.4%)	1,5 (6.8%)	0,1 (3.5%)	0,1 (3.6%)	0,4 (3.6%)	0,1 (3.8%)	0,2 (4.1%)	1,3 (6.0%)
III+V	$\times 10^9$ (A.U.$m^{-2}.L^{-1}$)	0,3 (13.3%)	0,4 (10.8%)	2,7 (11.8%)	0,5 (28.5%)	0,5 (18.0%)	1,9 (17.8%)	0,3 (14.5%)	0,7 (19.9%)	1,9 (9.0%)
Total	$\times 10^9$ (A.U.$m^{-2}.L^{-1}$)	2,4 (100%)	3,6 (100%)	22,6 (100%)	1,8 (100%)	2,9 (100%)	10,6 (100%)	2,0 (100%)	3,7 (100%)	21,1 (100%)

[1] M. Maaz, M. Yasin, M. Aslam, G. Kumar, A.E. Atabani, M. Idrees, F. Anjum, F. Jamil, R. Ahmad, A.L. Khan, G. Lesage, M. Heran, J. Kim, Anaerobic membrane bioreactors for wastewater treatment: Novel configurations, fouling control and energy considerations, Bioresource Technology. 283 (2019) 358–372. https://doi.org/10.1016/j.biortech.2019.03.061.
[2] L. Sanchez, M. Carrier, J. Cartier, C. Charmette, M. Heran, J.-P. Steyer, G. Lesage, Enhanced organic degradation and biogas production of domestic wastewater at psychrophilic temperature through submerged granular anaerobic membrane bioreactor for energy-positive treatment, Bioresource Technology. 353 (2022) 127145. https://doi.org/10.1016/j.biortech.2022.127145.
[3] C. Chen, M. Sun, J. Chang, Z. Liu, X. Zhu, K. Xiao, G. Song, H. Wang, G. Liu, X. Huang, Unravelling temperature-dependent fouling mechanism in a pilot-scale anaerobic membrane bioreactor via statistical modelling, Journal of Membrane Science. 644 (2022) 120145. https://doi.org/10.1016/j.memsci.2021.120145.
[4] C. Chen, W. Guo, H.H. Ngo, Advances in Granular Growth Anaerobic Membrane Bioreactor (G-AnMBR) for Low Strength Wastewater Treatment, (2016) 7.
[5] R. Chen, Y. Nie, Y. Hu, R. Miao, T. Utashiro, Q. Li, M. Xu, Y.-Y. Li, Fouling behaviour of soluble microbial products and extracellular polymeric substances in a submerged anaerobic membrane bioreactor treating low-strength wastewater at room temperature, Journal of Membrane Science. 531 (2017) 1–9. https://doi.org/10.1016/j.memsci.2017.02.046.
[6] C. Chen, W. Guo, H.H. Ngo, S.W. Chang, D. Duc Nguyen, P. Dan Nguyen, X.T. Bui, Y. Wu, Impact of reactor configurations on the performance of a granular anaerobic membrane bioreactor for municipal wastewater treatment, International Biodeterioration & Biodegradation. 121 (2017) 131–138. https://doi.org/10.1016/j.ibiod.2017.03.021.
[7] O.T. Iorhemen, R.A. Hamza, M.S. Zaghloul, J.H. Tay, Aerobic granular sludge membrane bioreactor (AGMBR): Extracellular polymeric substances (EPS) analysis, Water Research. 156 (2019) 305–314. https://doi.org/10.1016/j.watres.2019.03.020.
[8] W. Zhang, W. Liang, Z. Zhang, T. Hao, Aerobic granular sludge (AGS) scouring to mitigate membrane fouling: Performance, hydrodynamic mechanism and contribution quantification model, Water Research. 188 (2021) 116518. https://doi.org/10.1016/j.watres.2020.116518.
[9] O.T. Iorhemen, R.A. Hamza, J.H. Tay, Membrane fouling control in membrane bioreactors (MBRs) using granular materials, Bioresource Technology. 240 (2017) 9–24. https://doi.org/10.1016/j.biortech.2017.03.005.
[10] B. Zhang, D. Huang, Y. Shen, W. Yin, X. Gao, B. Zhang, W. Shi, Treatment of municipal wastewater with aerobic granular sludge membrane bioreactor (AGMBR): Performance and membrane fouling, Journal of Cleaner Production. 273 (2020) 123124. https://doi.org/10.1016/j.jclepro.2020.123124.
[11] I. Martin-Garcia, M. Mokosch, A. Soares, M. Pidou, B. Jefferson, Impact on reactor configuration on the performance of anaerobic MBRs: Treatment of settled sewage in temperate climates, Water Research. 47 (2013) 4853–4860. https://doi.org/10.1016/j.watres.2013.05.008.
[12] W. Zhang, F. Jiang, Membrane fouling in aerobic granular sludge (AGS)-membrane bioreactor (MBR): Effect of AGS size, Water Research. 157 (2019) 445–453. https://doi.org/10.1016/j.watres.2018.07.069.
[13] C. Xu, Z. Li, J. Wang, Z. Zhou, Exposure to stressful conditions alters the properties and fouling behavior of suspended microparticles in anaerobic processes, Journal of Environmental Chemical Engineering. 9 (2021) 106782. https://doi.org/10.1016/j.jece.2021.106782.a

[14] Y. Yao, Z. Zhou, D.C. Stuckey, F. Meng, Micro-particles—A Neglected but Critical Cause of Different Membrane Fouling between Aerobic and Anaerobic Membrane Bioreactors, ACS Sustainable Chem. Eng. 8 (2020) 16680–16690. https://doi.org/10.1021/acssuschemeng.0c06502.
[15] K.M. Wang, N.M. Garcia, A. Soares, B. Jefferson, E.J. McAdam, Comparison of fouling between aerobic and anaerobic MBR treating municipal wastewater, H2Open Journal. 1 (2018) 131–159. https://doi.org/10.2166/h2oj.2018.109.
[16] S. Vinardell, L. Sanchez, S. Astals, J. Mata-Alvarez, J. Dosta, M. Heran, G. Lesage, Impact of permeate flux and gas sparging rate on membrane performance and process economics of granular anaerobic membrane bioreactors, Science of The Total Environment. 825 (2022) 153907. https://doi.org/10.1016/j.scitotenv.2022.153907.
[17] K.M. Wang, D. Cingolani, A.L. Eusebi, A. Soares, B. Jefferson, E.J. McAdam, Identification of gas sparging regimes for granular anaerobic membrane bioreactor to enable energy neutral municipal wastewater treatment, Journal of Membrane Science. 555 (2018) 125–133. https://doi.org/10.1016/j.memsci.2018.03.032.
[18] A. Alphenaar, Anaerobic granular sludge: characterization, and factors affecting its functionning, Wageningen Agricultural University, 1994. https://edepot.wur.nl/202099.
[19] J. O'Reilly, C. Lee, F. Chinalia, G. Collins, T. Mahony, V. O'Flaherty, Microbial community dynamics associated with biomass granulation in low-temperature (15°C) anaerobic wastewater treatment bioreactors, Bioresource Technology. 101 (2010) 6336–6344. https://doi.org/10.1016/j.biortech.2010.03.049.
[20] C. Chen, W.S. Guo, H.H. Ngo, Y. Liu, B. Du, Q. Wei, D. Wei, D.D. Nguyen, S.W. Chang, Evaluation of a sponge assisted-granular anaerobic membrane bioreactor (SG-AnMBR) for municipal wastewater treatment, Renewable Energy. 111 (2017) 620–627. https://doi.org/10.1016/j.renene.2017.04.055.
[21] P. Le Clech, B. Jefferson, I.S. Chang, S.J. Judd, Critical flux determination by the flux-step method in a submerged membrane bioreactor, Journal of Membrane Science. 227 (2003) 81–93. https://doi.org/10.1016/j.memsci.2003.07.021.
[22] APHA, AWWA, WEF, eds., Standard methods: for the examination of water and wastewater, 20. ed, American Public Health Association, Washington, DC, 1998.
[23] R. Zepp, W. Sheldon, M.A. Moran, Dissolved organic fluorophores in southeastern US coastal waters: Correction method for eliminating Rayleigh and Raman scattering peaks in excitation-emission matrices, Marine Chemistry. 89 (2004) 15–36. https://doi.org/10.1016/j.marchem.2004.02.006.
[24] C. Jacquin, G. Lesage, J. Traber, W. Pronk, M. Heran, Three-dimensional excitation and emission matrix fluorescence (3DEEM) for quick and pseudo-quantitative determination of protein- and humic-like substances in full-scale membrane bioreactor (MBR), Water Res. 118 (2017) 82–92. https://doi.org/10.1016/j.watres.2017.04.009.
[25] M. Dubois, K. Gilles, J.K. Hamilton, P.A. Rebers, F. Smith, A Colorimetric Method for the Determination of Sugars, Nature. 168 (1951) 167–167. https://doi.org/10.1038/168167a0.
[26] OliverH. Lowry, NiraJ. Rosebrough, A.L. Farr, RoseJ. Randall, Protein measurement with the Folin phenol reagent, Journal of Biological Chemistry. 193 (1951) 265–275. https://doi.org/10.1016/S0021-9258(19)52451-6.
[27] J. Wu, Z.Y. Lu, J.C. Hu, L. Feng, J.D. Huang, X.S. Gu, Disruption of granules by hydrodynamic force in internal circulation anaerobic reactor, Water Sci Technol. 54 (2006) 9–16. https://doi.org/10.2166/wst.2006.868.
[28] Z. Zhou, Y. Tao, S. Zhang, Y. Xiao, F. Meng, D.C. Stuckey, Size-dependent microbial diversity of sub-visible particles in a submerged anaerobic membrane bioreactor

(SAnMBR): Implications for membrane fouling, Water Research. 159 (2019) 20–29. https://doi.org/10.1016/j.watres.2019.04.050.

[29] D. Jeison, J.B. van Lier, Cake layer formation in anaerobic submerged membrane bioreactors (AnSMBR) for wastewater treatment, Journal of Membrane Science. 284 (2006) 227–236. https://doi.org/10.1016/j.memsci.2006.07.035.

[30] A. Massé, M. Spérandio, C. Cabassud, Comparison of sludge characteristics and performance of a submerged membrane bioreactor and an activated sludge process at high solids retention time, Water Research. 40 (2006) 2405–2415. https://doi.org/10.1016/j.watres.2006.04.015.

[31] L. Böhm, A. Drews, H. Prieske, P.R. Bérubé, M. Kraume, The importance of fluid dynamics for MBR fouling mitigation, Bioresource Technology. 122 (2012) 50–61. https://doi.org/10.1016/j.biortech.2012.05.069.

[32] E. Nguyen Cong Duc, L. Fournier, C. Levecq, B. Lesjean, P. Grelier, A. Tazi-Pain, Local hydrodynamic investigation of the aeration in a submerged hollow fibre membranes cassette, Journal of Membrane Science. 321 (2008) 264–271. https://doi.org/10.1016/j.memsci.2008.05.001.

[33] S. Chellam, M.R. Wiesner, Particle Back-Transport and Permeate Flux Behavior in Crossflow Membrane Filters, Environ. Sci. Technol. 31 (1997) 819–824. https://doi.org/10.1021/es9605228.

[34] E. Tardieu, A. Grasmick, V. Geaugey, J. Manem, Hydrodynamic control of bioparticle deposition in a MBR applied to wastewater treatment, Journal of Membrane Science. 147 (1998) 1–12. https://doi.org/10.1016/S0376-7388(98)00091-X.

[35] H. Lin, W. Peng, M. Zhang, J. Chen, H. Hong, Y. Zhang, A review on anaerobic membrane bioreactors: Applications, membrane fouling and future perspectives, Desalination. 314 (2013) 169–188. https://doi.org/10.1016/j.desal.2013.01.019.

[36] W.J. Gao, H.J. Lin, K.T. Leung, H. Schraft, B.Q. Liao, Structure of cake layer in a submerged anaerobic membrane bioreactor, Journal of Membrane Science. 374 (2011) 110–120. https://doi.org/10.1016/j.memsci.2011.03.019.

[37] J. Altmann, S. Ripperger, Particle deposition and layer formation at the crossflow microfiltration, Journal of Membrane Science. 124 (1997) 119–128. https://doi.org/10.1016/S0376-7388(96)00235-9.

[38] H. Yang, Z. Li, Y. Chen, Z. Zhou, Role of microparticles in membrane fouling from acidogenesis to methanogenesis phases in an anaerobic baffled reactor, Science of The Total Environment. 806 (2022) 150663. https://doi.org/10.1016/j.scitotenv.2021.150663.

[39] Z. Yang, Q.N. Tran, X. Jin, Ultrafiltration of aerobic granular sludge bioreactor effluent: Fouling potentials and properties, Journal of Water Process Engineering. 47 (2022) 102805. https://doi.org/10.1016/j.jwpe.2022.102805.

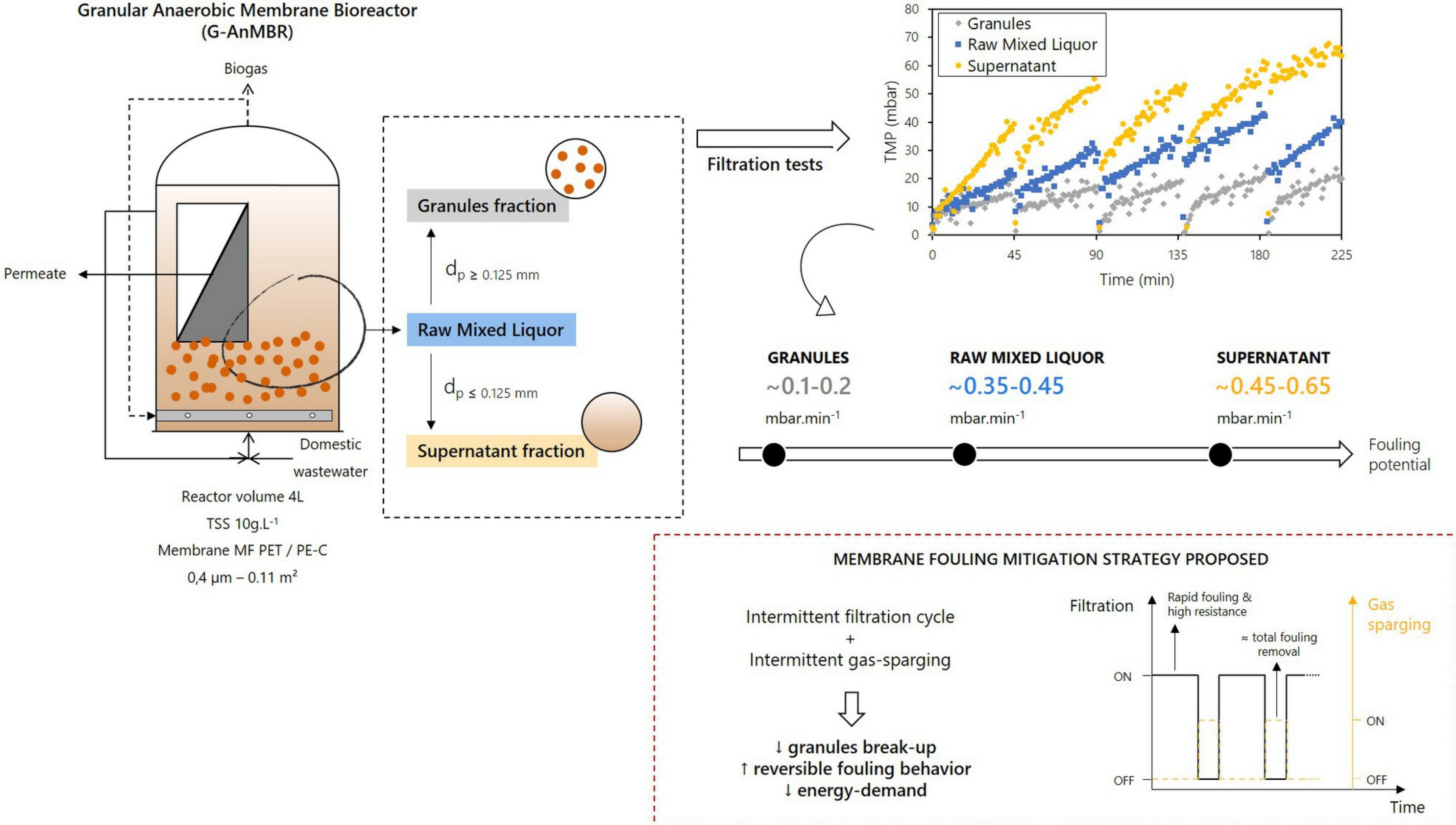
Granular Anaerobic Membrane Bioreactor (G-AnMBR)
Biogas
Permeate
Domestic wastewater
Reactor volume 4L
TSS 10g.L-1
Membrane MF PET / PE-C
0,4 µm – 0.11 m²
Granules fraction
dp ≥ 0.125 mm
Raw Mixed Liquor
dp ≤ 0.125 mm
Supernatant fraction
Filtration tests
Granules
Raw Mixed Liquor
Supernatant
TMP (mbar)
Time (min)
GRANULES
~0.1-0.2
mbar.min-1
RAW MIXED LIQUOR
~0.35-0.45
mbar.min-1
SUPERNATANT
~0.45-0.65
mbar.min-1
Fouling potential
MEMBRANE FOULING MITIGATION STRATEGY PROPOSED
Intermittent filtration cycle
+
Intermittent gas-sparging
↓ granules break-up
↑ reversible fouling behavior
↓ energy-demand
Filtration
Rapid fouling & high resistance
≈ total fouling removal
Gas sparging
ON
OFF
Time